WHEEL PJ

Precambrian World 2023 in Egypt

6th International Geoscience Symposium

2023

2nd International WHEEL seminar

2023

December 8 (Fri) - 9 (Sat)

Field trip: December 9-13

at NRIAG

National Research Institute of Astronomy and Geophysics

--Modern, Past and Future of Earth Recored: geologic, oceanic, biogenic evidences during 4.6Ga--

http://wheelaa.jp

adress: EL Marsad Street 1, Helwan, Cairo
Telephone: (+202) 255 41100 - 255 49780
Post No: 11421 Box:138

JSPS 日本学術振興会 Japan Society for the Promotion of Science

研究拠点形成事業 Core-to-Core Program Asia-Africa Science Platforms

科研費 KAKENHI

KYUSHU UNIVERSITY

地球掘削科学国際研究拠点 Joint Usage/Research Center for Drilling Earth Science

茨城大学 Ibaraki University

National Museum of Nature and Science (geology)
National Institute of Polar Research (SHRIMP Lab)

Tectonic, sedimentary history and iron formation of the Neoproterozoic metavolcanic–volcaniclastic sequence of the El-Dabbah Group, Central Eastern Desert, Egypt.

Shoichi Kiyokawa [1,2,3]
1. Department of Earth and Planetary Sciences, Kyushu University, Fukuoka, Japan.
2. Center for Advanced Marine Core Research, Kochi University
3. Department of Geology, University of Johannesburg
kiyokawa@geo.kyushu-u.ac.jp

1. Introduction

The Eastern Desert in Egypt was situated northern portion of the East African Orogeny (Fitz et al., 2013) which was escaped potion of the collision between East and West Gondowana. It contains well preserved accreted island-arc sections, granitic rocks and exhumed metamorphic rocks. Especially, the Central East Desert (CED) well preserved low-grade assemblage of suprastructural unit (eg. El-Shazly and Khalil, 2016).

The El-Dabbah Group is a >5km-thick metavolcanic – volcaniclastic sequence containing iron formation in the Nubian Shield, Central Eastern Desert, Egypt. It preserves a sequence of lower-greenschist-facies rocks that are little deformed, overlain by subaerial sedimentary strata deposited in strike-slip basins.

Based on detailed mapping, here our group reconstructed the stratigraphic–tectonic history of the El-Dabbah Group and surrounding sedimentary basins. The formation was deposited near an island-arc ocean floor setting. It contains several banded iron formations within volcaniclastic sequence. The subaerial sedimentary strata of the Atshan Formation and Hammamat Group, which are well preserved along strike-slip faults, unconformably overlie the El-Dabbah Group. This presentation is based on the Kiyokawa et al, 2020 a,b.

2. Results

2-1 Geological flame work

the Wadi El-Dabbah area, we identified five fault systems (F_1 to F_5) and subdivided into four uneven, fault-bounded domains: the northeast (NE), southeast (SW), northwest (NW), and southwest (SW) domains.

2-2 Age dating: New geochronological data reveal crystallization ages of 638.1 ± 2.9 Ma for granite intruded into the El-Dabbah Group and 659.6 ± 3.0 Ma for quartz porphyry intruded into the Atshan Formation. Detrital zircon ages from the base of the Hammamat Group show peaks at 650, 680, and 790 Ma.

2-3 Stratigraphic reconstructed sequence

El-Dabbah Group is divided into Lower ED, Middle ED, and Upper ED formations (Fig. 6). Total thickness of this group is approximately 7500 m.

Lower ED Formation consists of coarse-grained massive basaltic rocks interbedded with thin layers of volcaniclastic rocks and few fine grain dorelite.

Middle ED Formation contains numerous massive lava, pillow lava, and metavolcanic units interbedded with fine-grained tuff beds, iron-rich beds and banded iron formation (BIF).

Upper ED Formation comprises volcaniclastic sediments, minor pillow lavas, and mainly reworked, cross-stratified volcaniclastic rocks.

3. Conclusion

Tectonic flame work

Three stages of sedimentation and structural deformation have been identified in this area. Stage 1 involved island arc volcanogenic sedimentation and accretion-related thrust deformation (D_1: 700–680 Ma). Stage 2 was a transtensional phase related to the formation of a subaerial basin (Atshan Formation), normal faulting, and strong strike-slip deformation (D_2: 680–630 Ma). Granites were intruded during this stage. Stage 3 involved orogenic collapse and strike-slip deformation of the Najd fault system (D_3: 620–580 Ma), which resulted in subaerial sedimentation of the Hammamat Group in pull-apart basins. The formation of the basins was associated with continuing extensional deformation that affected the Hammamat Group (D_4: <580 Ma).

References

El-Shazly A.K., Khalil K.I., 2016. Metamprphic and geochronologic constraints on the tectonic evolution of the Central Eastern Desert of Egypt. Precambrian. Research, 283, 144-168.

Fritz H., et al., 2013. Orogen styles in the East African Orogen: A review of the Neoproterozoic to Cambrian tectonic evolution. Journal of African Earth Sciences, 86, 65-106.

Kiyokawa, S., Suzuki, T., Horie, K., Takehara, M., El-Dokounyd, H.A., Dawoud, M., and Abuelhasan, M.M., 2020a, Tectonic and sedimentary history of the Neoproterozoic metavolcanic–volcaniclastic rocks of the El-Dabbah Group, Central Eastern Desert, Egypt. Journal of African Earth Sciences. v. 165, p. 1-16,

Kiyokawa, S., Suzuki, T., El-Dokounyd, H.A., Dawoud, M., and Abuelhasan, M.M. 2020b. Stratigraphy, petrology, and geochemistry of a Neoproterozoic banded iron sequence in the El-Dabbah Group, Central Eastern Desert, Egypt. Journal of African Earth Sciences. v. 168, p. 1-17.

U–Pb geochronology and Hf isotope systematics of detrital zircon from the basal part of the late Ediacaran sedimentary sequence of the Moldova-Podillya basin (SW Baltica): implications for glacial vs. alluvial origin

Ion Francovschi[1,2,3], Leonid Shumlyanskyy[4,5], Volodymyr Grytsenko[6], Adam Hoffmann[3], Andrey Bekker[3,7]

1. University of Bucharest, Faculty of Geology and Geophysics, Bucharest, Romania
2. Moldova State University, Institute of Geology and Seismology, Chișinău, Republic of Moldova
3. Department of Earth & Planetary Sciences, University of California, Riverside, USA

frankovski.ww@gmail.com

4. Institute of Geological Sciences, Polish Academy of Sciences (ING PAN), Kraków, Poland
5. School of Earth and Planetary Sciences, Curtin University, Australia
6. National Museum of Natural History, National Academy of Sciences of Ukraine, Kyiv, Ukraine
7. Department of Geology, University of Johannesburg, South Africa

1. Introduction

The Neoproterozoic is marked by two long-lasted, global, Snowball Earth glaciations, Sturtian and Marinoan, between ca. 715 and 660 Ma and ca. 639 and 635 Ma, respectively, and a shorter-lived, potentially regional Gaskiers glaciation at ca. 580-579 Ma [1, 2]. However, a number of locally, and, sometimes regionally, developed sedimentary units worldwide has been interpreted to record sea-level, local to regional glaciations during the Ediacaran and Early Cambrian [3, 4]. Some of these units poorly outcrop, were affected by deformation and metamorphism, lack definitive sedimentologic textures and structures to support their glacial origin, and are poorly dated. Their sedimentological features as well as age constraints are thus often insufficient to resolve whether they have indeed glacial origin and cluster into well-defined glacial time intervals. Detrital zircon geochronology could resolve between heterogeneous, extensive provenance, required by glacial processes, and homogenous, local provenance, corresponding to alluvial settings. Herein, we use trends in detrital zircon age distribution patterns from the lowermost, late Ediacaran sedimentary succession of the Moldova-Podillya basin (SW Baltica) to constrain the provenance of the late Ediacaran Volyn Group sediments.

2. Results and discussion

Detrital zircon grains from one sample (Bakhtyn beds, Volyn Group) yielded Mesoarchean ages of ca. 2970 and 2800 Ma, and Paleoproterozoic ages of 2061 ± 8 Ma. Paleoproterozoic zircons have εHf values varying from 3 to -4.6, while two Mesoarchean zircon crystals also have εHf values close to the CHUR (1.5 and -4). Two other samples from the same formation yielded two age groups: Paleoproterozoic ages varying from 2217 ± 11 Ma to 2039 ± 5 Ma, and Mesoarchean to Neoarchean ages ranging from 2882 ± 24 to 2538 ± 28 Ma. Archean zircons reveal negative εHf values in the range from -4.8 to -26.7. Higher in the sedimentary sequence, two samples from the Lomoziv beds, Mohyliv-Podilsk Group reveal ages from 2167 ± 8 Ma to 2002 ± 12 Ma.

Geochronological and Hf isotope analyses on detrital zircons from the basal part of the late Ediacaran sequence of the Moldova-Podillya basin (SW Baltica) indicate that the late Ediacaran Bakhtyn beds, Volyn Group, contain zircons associated with proximal sources, derived from the crystalline basement and do not display a distinct "alien" signature. Consequently, these diamictites are of alluvial origin. We suggest that detrital zircon geochronology holds an untapped potential to test glacial origin for units that are otherwise poorly sedimentologically and geochronologically characterized.

References

Macdonald, F.A., Schmitz, M.D., Crowley, J.L., Roots, C.F., Jones, D.S., Maloof, A.C., Schrag, D.P., 2010a. Calibrating the Cryogenian. *Science* **327(5970)**, 1241–1243.

Rooney, A.D., Strauss, J.V., Brandon, A.D., Macdonald, F.A., 2015. A Cryogenian chronology: Two long-lasting synchronous Neoproterozoic glaciations. *Geology* **43**, 459–462.

Chumakov, N.M., 2011. Glacial deposits of the Baykonur Formation, Kazakhstan and Kyrgyzstan. Chapter 26. In: Arnaud, E., Halverson, G. P., Shields-Zhou, G. (eds) The Geological Record of Neoproterozoic Glaciations. Geological Society, London, **Memoirs** *36*, 303–307.

Wang, R., Shen, B., Lang, X., Wen, B., Mitchell, R.N., Ma, H., Yin, Z., Peng, Y., Liu, Y., Zhou, C., 2023. A Great late Ediacaran ice age. **National Science Review** *10(8)*, nwad117.

GEOCHEMISTRY AND PETROGENESIS OF LATE NEOPROTEROZOIC NUWEIBI AND ATAWI RARE METALS BEARING GRANITES, CENTRAL EASTERN DESERT, EGYPT

El-Dokouny, H.A.[1], Watanabe, Y.[2], Mahmoud, A.S.[3], and Dawoud, M.[4],

1. Geology Department, Faculty of Science, Menoufia University, Egypt
   hanaa.abdelmoneam1@science.menoufia.edu.eg
   hanaaabdelnaby4@gmail.com
2. Department of Earth Resource Science, Graduate School of International Resource Sciences, Akita University, 1-1, Tegata-Gakuenmachi, Akita, 010-8502 Japan
   y-watanabe@gipc.akita-u.ac.jp
3. Geology Department, Faculty of Science, Fayoum University, Egypt
   halim.geologist@mail.ru
4. Geology Department, Faculty of Science, Menoufia University, Egypt
   dawoud_99@yahoo.com

1. Introduction

The Nuweibi and Atawi rare-metal granites are part of the Arabian-Nubian Shield's (ANS) basement complex. Granitic rocks were emplaced in the late stages of the formation of the ANS crust in Egypt during the Late Neoproterozoic. They are extensive in the Eastern Desert of Egypt, including syn- to late collisional granitoids (older phase of 850-614 Ma) and postorogenic to anorogenic granites; A-type granites (younger phase of 610-550 Ma; Stern, 1994). A-type granitic rocks have considerable economic value due to their high concentrations of rare metals, notably the albite granite variety (Helba et al., 1997; Heikal et al., 2019; Shahin et al., 2021).We have chosen two granitic plutons (Nuweibi albite granite; NAG and Atawi granite; AG) that are thought to be evolutionary successive and overlapped to shed the light and remove the mystery on the paragenesis and the contribution of magmatic mineral fractionation and late-magmatic fluid stage processes in the enrichment of rare metals.

2. Results

NAG has intruded the metasediments and grey granites. Stockscheider marginal pegmatites, quartz-amazonite veins found close to the contact accompanying with greisenization (Mohamed, 2012). AG intrudes the metasedimentary and metavolcanic rocks with sharp intrusive contacts. It is altered in the northern margin of the pluton, near to the contact with the metasediments where in the western part it is cut by N-S quartz-fluorite-calcite veins dipping ~80˚ E.

NAG consists of albite (Anorthite content=2), quartz, orthoclase, minor microcline and muscovite with Fe-Mn oxides, garnet and few minute zircons as accessory minerals. AG is composed mostly of quartz, orthoclase perthite, albite (An=4:10), microcline and highly altered mica (mainly biotite ± muscovite) with opaque minerals, zircon, titanite and fluorite as accessory minerals.

Both are low-P_2O_5 metaluminous to peraluminous granitic magma. The chemical features of NAG and AG as Na_2O + K_2O, FeO^t/MgO, Ga, Nb and Ta high concentrations are compatible with anorogenic within plate tectonic setting. However, NAG has higher concentration of Al_2O_3, Na_2O, MnO, Ga, Rb, Hf and Ta and lower concentrations of SiO_2, TiO_2, $Fe_2O_3^t$, MgO, CaO, K_2O, P_2O_5, Ba, Zr, Y, Sn, W, F and REEs. NAG shows obvious enrichment of HREEs relative to LREEs, negative Eu anomaly and tetrad effect. On the other hand, AG has a higher concentration of REEs and it is slightly enriched in LREEs relative to HREEs with negative Eu anomaly. NAG shows very low ratios of Eu/Eu* (0.17-0.3), (La/Yb)n (0.06-0.4), Nb/Ta (0.44-1.09), Zr/Hf (1.84-2.61), K/Rb (66.8-109.9) and Y/Ho ratios (2.9-6.3) together with high Sr/Eu (160-440). On the other hand, AG shows chondritic or almost chondritic Nb/Ta (5.5-15.9), Zr/Hf (14.8-28.6), Y/Ho (26.2-45), K/Rb (99.24-346.28) and Sr/Eu (56.6-520) ratios indicating the lower effect of late magmatic fluid-rock interaction compared to NAG.

3. Discussion

The absence of mafic lithologies associated NAG as well as absence of mafic xenoliths or enclaves in AG and NAG, peraluminous character, K/Rb and K/Ba ratios suggest a significant contribution of upper crustal sources and exclude a pure mantle source for these granitic magmas. This interpretation is supported by high $\delta^{18}O$ (Be'eri-Shlevin et al., 2009) and the presence of inherited zircons with ages near 740 and 1790 Ma (Ali et al., 2009) of some A-type granites in the Nubian Shield,

The geochemical data from NAG and AG whole rock analyses indicate that the ore elements were incompatible during magma crystallization and crystallized late in the magma's history in the presence of a volatile-rich fluid. The following series of events explains proposed history in detail:

1) Prolonged formation of major mineral constituents (quartz and feldspar including magmatic albite, orthoclase, and few of microcline).

2) Trace element- rich phase enriched in volatile elements (H_2O, F, and CO_2) "late-stage magmatic fluid" evolved from the magma. Trace elements can be transported in this phase as a result of complexing with F and other agents causing decreasing of the crystallization temperature of accessory minerals and permitting trace elements (Ta, Nb, Rb, Zr, W and REEs) to behave as incompatible elements.

3) Accessory minerals crystallised from this phase interstitially between the major mineral phases as in Atawi. REEs may be fixed in zircon and titanite moreover, the concentration of F is high enough to fix Ca forming fluorite which are common in the studied AG and veins cut through.

4) The residual fluids enriched in alkalis interact with the early stage crystallized minerals forming late-stage albite after K-feldspar (orthoclase± microcline) leading to small scale albitization in Atawi and larger scale albitization in Nuweibi.

5) K liberated from albitization of K-feldspar consumed by greisenization forming muscovite after biotite and feldspar in Nuweibi leading to SiO_2 decreasing and Na_2O, Al_2O_3 increasing (similar to Mueilha rare metal granite; Seddik et al., 2020), meanwhile, Ca, CO_2, F and Si in the fluid formed Quartz-fluorite-calcite veins cutting through the AG.

6) The fluid at this stage becomes depleted in F, Ca and REEs due to consuming by accessory minerals crystallised in Atawi or may be due to getting out of fluid enriched in

these elements from the system (Dawoud, 2004). Thereby NAG lacks accessory minerals encompassing the REEs, F and Ca; only very few garnet and zircon is found.

7) Severe greisenization in late stages in Nuweibi liberated Fe and Mn as a result of biotite decomposition forming Mn-Fe oxide as patches, dendritic clusters, filling of joints and tinny cover along the boundaries of grain. Moreover, greisen, stockscheider pegmatites, and quartz-amazonite veins have been formed at the contact between the albite granite and its country rocks.

References

Ali, B. H, Wilde, S. and Gabr, M. (2009). Granitoid evolution in Sinai, Egypt, based on precise SHRIMP U–Pb zircon geochronology. Gondwana Research, 15(1), 38-48.

Be’eri-Shlevin Y., Katzir Y. and Valley, J. W. (2009). Crustal evolution and recycling in a juvenile continent: oxygen isotope ratio of zircon in the northern Arabian Nubian Shield. Lithos, 107(3-4), 169-184.

Dawoud, M., (2004). The nature and origin of U-bearing fluids as revealed from zircon alteration: examples from the Gattarian granites of Egypt. Sixth International Conference of Geochemistry, Alexandria University, I-B, 875-891

Heikal, M. T. S., Khedr, M. Z., Abd El Monsef, M. and Gomaa, S. R. (2019). Petrogenesis and geodynamic evolution of neoproterozoic Abu Dabbab albite granite, central Eastern Desert of Egypt: petrological and geochemical constraints. Journal of African Earth Sciences, 158, 103518.

Helba, H., Trumbull, R. B., Morteani, G., Khalil, S. O., and Arslan, A. (1997). Geochemical and petrographic studies of Ta mineralization in the Nuweibi albite granite complex, Eastern Desert, Egypt. Mineral Deposita, 32, 164-179.

Shahin, H. A., Emad, B. M. and Masoud, M.S. (2021). Uranium and rare metal mineralization in the El Sela and Qash Amir granitic intrusions, south Eastern Desert, Egypt. Journal of Asian Earth Sciences: X, 100066

Stern, R. J, (1994). ARC Assembly and Continental Collision in the Neoproterozoic East African Orogen: Implications for the Consolidation of Gondwanaland. Annual Review of Earth and Planetary Sciences, 22(1), 319-351.

COMPARING PRECAMBRIAN GRANULAR IRON FORMATIONS AND PHANEROZOIC OOLITIC IRONSTONES – SIMILAR BEASTS WITH DIFFERENT ORIGINS?

Alex Kovalick[1], Andrey Bekker[1], Andrew Heard[2], Maria Prokopenko[2], and Robert Gaines[2]

1. Department of Earth & Planetary Sciences, University of California-Riverside, Riverside, California, United States of America
fkova001@ucr.edu
2. Woods Hole Oceanographic Institute, Woods Hole, Massachusetts, United States of America
3. Geology Department, Pomona College, Clairemont, California, United States of America

1. Introduction

Paleoproterozoic Granular Iron Formations (GIFs) and Phanerozoic ironstones (ISs) have been episodically deposited since the Great Oxidation Episode (ca. 2.4-2.1 Ga) (Bekker et al., 2013). Although each share similar mineralogy, sedimentary textures, and depositional environments, different iron sources have been inferred for GIFs and ISs. It is generally recognized that Paleoproterozoic GIF deposition was episodic, synchronous with Volcanogenic Massive Sulfide deposition and submarine Large Igneous Provinces emplacements that caused short-term perturbations to the redox state of the oceans (Bekker et al, 2013). Therefore, Fe^{2+} for GIF deposition is thought to be sourced from the deep oceans, where hydrothermal fluids leached Fe and Mn from volcanics (Isley & Abbott, 1999). In contrast, Fe^{2+} for ISs is assumed to be sourced from continents during periods of intense chemical weathering (Van Houten & Battacharyya, 1982). Although the Proterozoic and Paleozoic deep oceans were both anoxic and ferruginous at least episodically, smaller reducing submarine hydrothermal fluxes and higher seawater sulfate content in the Paleozoic may have supported a stronger seawater oxidant buffer preventing long-distance Fe transport. Continental weathering has therefore been considered a viable process to supply Fe^{2+} to the oceans for IS deposition. This raises the potential of different Fe precipitation mechanisms in their formation. Using a combination of paleontological and geochemical methods, we investigate the Fe source and precipitation mechanisms involved in the formation of GIFs from the ca. 1.88 Ga Gibraltar Formation and ironstones from the Carboniferous Amsden Formation (ca. 320 Ma).

2. Results

The Gibraltar Formation GIFs preserve positive Eu anomalies similar to other GIFs deposited at ca. 1.88 Ga, which is consistent with a hydrothermal origin for Fe2+(aq). Redox-sensitive rare earth element compositions (REE; i.e., Ce anomaly, LREE/HREE, Y/Ho) alongside a large range of Fe-isotope values indicate the Gibraltar Formation GIFs precipitated as Fe-oxyhydroxide minerals via partial Fe-oxidation of Fe2+(aq). These findings are supported by filamentous microfossils resembling modern, microaerophilic, iron-oxidizing bacteria, which non-quantitatively oxidize Fe2+(aq) from solution, enabling a large range of Fe-isotope values in the resulting sediments. Similarly, the Amsden Formation ironstones record large positive Eu anomalies, and REE compositions and Fe-isotope values in co-occurring hematite and chamosite (Fe-silicate) oolites that indicate partial Fe-oxidation at a redoxcline.

3. Discussion

These findings indicate that, despite significant paleoenvironmental difference between the Proterozoic and Phanerozoic, the Amsden Formation ironstone was deposited in a similar fashion to Paleoproterozoic GIFs via long-distance transport and upwelling of deep-ocean ferruginous waters in association with intense submarine hydrothermal activity that fueled slow, partial Fe-oxidation along a redoxcline in a shallow-marine setting.

References

Bekker, A., Planavsky, N.J., Krapež, B., Rasmussen, B., Hofmann, A., Slack, J.F., Rouxel, O.J., Konhauser, K.O., 2014. Iron Formations: Their Origins and Implications for Ancient Seawater Chemistry, in: Treatise on Geochemistry. Elsevier, pp. 561–628.

Isley, A. & Abbott, D. Plume-related mafic volcanism and the deposition of banded iron formation. Journal of Geophysical Research 104, 15461-15477 (1999).

Van Houten, F.B., Bhattacharyya, D.P., 1982. Phanerozoic Oolitic Ironstones--Geologic Record and Facies Model. Annu. Rev. Earth Planet. Sci. 10, 441–457.

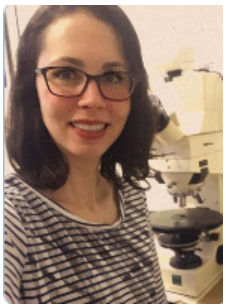

OXYGEN ISOTOPE SIGNATURE OF IRON-FORMATION-HOSTED ORE

Flávia Cristina Silveira Braga[1], Carlos Alberto Rosière[1], Andreas Pack[2], Steffen Hagemann[3] and João Orestes Schneider Santos[3]

1. Department of Geology, Universidade Federal de Minas Gerais, Belo Horizonte, Brazil
flaviacsbraga@gmail.com, crosiere@gmail.com
2. Georg-August-Universität, Göttingen, Germany
andreas.pack@geo.uni-goettingen.de
3. Centre for Exploration Targeting, University of Western Australia, Perth, WA, Australia
steffen.hagemann@uwa.edu.au
4. Universidade do Estado do Amazonas, Manaus, AM, Brazil
orestes1@uol.com.br

1. Introduction

Iron formation (IF)-hosted high-grade iron deposits represent a significant global metal source. Upper amphibolite facies Lake-Superior-type IFs contain magnetite-hematite orebodies associated with pegmatite remobilized from alkaline granitic intrusions on the eastern margin of the São Francisco Craton, bordering the Ediacaran-Cambrian Brasiliano Orogenic belt in Brazil. The oxygen isotope composition (δ18O) of different generations of iron oxides (hematite, magnetite) collected from iron formation, high-grade bodies, and veins reveals a distinct signature for this type of deposit. These results provide a clearer insight on the evolution of IF-hosted ore, revealing a complex interplay of geological elements such as magmatic intrusion, metamorphic processes, and other specific environmental conditions that characterize a new magmatic-hydrothermal type of ore.

2. Results

The $\delta^{18}O_{mineral}$ values range from -1.6 to 8.1‰, with IF iron oxides exhibiting the heaviest signatures (1.7 to 8.1‰), followed by quartz and pegmatite veins (1.8 to 5.0‰) and ore bodies (-1.6 to 2.6‰).

The study employed fractionation curves to calculate $\delta^{18}O_{fluid}$ values in equilibrium with the different iron oxides, considering fluid inclusion homogenization temperatures of 150 and 350 °C. The values obtained were based on curves from Yapp (1990), Zheng (1991), Zheng and Simon (1991), Bao and Koch (1999). To the temperature of 150 °C the calculated $\delta^{18}O_{fluid}$ intervals are: 4.6 – 19.6 to IF, 1.3-14.1 to high-grade ore and 4.6-14.6 to pegmatite and quartz veins. To the temperature of 350 °C the calculated $\delta^{18}O_{fluid}$ intervals are: 9.0 – 18.0 to IF, 3.5-12.5 to high-grade ore and 6.8-13.2 to pegmatite and quartz veins.

3. Discussion

The oxygen isotope profile in the studied iron formation-hosted deposits demonstrates a consistent decline in $\delta^{18}O_{mineral}$ values from the IF (1.7 to 8.1‰) to high-grade ore (-1.6 to 2.6‰), aligning with a common trend in this mineralization type. Notably, these specific cases reveal the evident influence of magmatic fluids, resulting in a relatively higher oxygen isotope signature compared to most global hypogene IF high-grade ores. This elevated signature approaches values found in magnetite-apatite ores of the Kiruna type.

Our calculated $\delta^{18}O_{fluid}$ values for iron oxides in high-grade ore and veins, using Yapp (1990) and Bao and Koch (1999) equations, align within the range of magmatic waters of Taylor (1979), between +5.5 to +10.0‰.

The $\delta^{18}O$ data provided by the iron oxides serves as an indicative marker for the gradual involvement of magmatic fluids in the mineralization process. This phenomenon is attributed to the tectonic reworking of consolidated sialic crust, associated with anatectic melting during a continental collision. This interpretation is substantiated by supporting evidence from tectonic, geochemical thermo-barometric, and petrographic data.

References

Bao, H., & Koch, P. L. (1999). Oxygen isotope fractionation in ferric oxide-water systems: Low temperature synthesis. *Geochim. Cosmochim. Acta* **63**, 599–613.

Taylor, H. P. (1979). Oxygen and Hydrogen isotope relationship in Hydrothermal mineral deposits, in: Barnes, H.L. (Ed.), Geochemistry of Hydrothermal Ore Deposits. The Pennsylvania State University, pp. 236–277.

Yapp, C. J. (1990). Oxygen isotopes in iron (III) oxides. *Chemical* **85**, 329–335.

Zheng, Y. F. (1991). Calculation of oxygen isotope fractionation in metal oxides. *Geochim. Cosmochim. Acta* **55**, 2299–2307.

Zheng, Y. F., & Simon, K. (1991). Oxygen isotope fractionation in hematite and magnetite: A theoretical calculation and application to geothermometry of metamorphic iron-formations. *European Journal of Mineralogy* **3**, 877–886.

IN SEARCH OF THE EVENT-BASED DEFINITION FOR THE ARCHEAN-PROTEROZOIC BOUNDARY

Andrey Bekker[1]

1. Department of Earth & Planetary Sciences, University of California, Riverside CA 92521 USA; andreyb@ucr.edu

There is a growing interest to base the Archean-Proterozoic boundary on the synchronous and potentially global surface event. The rise of atmospheric oxygen in the early Paleoproterozoic closely followed the assembly and emergence of large landmasses and associated emplacement of Large Igneous Provinces (LIPs), was bracketed by 3 to 4 Snowball Earth events, and led to the largest and longest positive carbon isotope excursion in seawater composition in Earth's history, the Lomagundi Event (LE). Since each of these events could be globally synchronous and widespread, they hold an eminent potential to define a GSSP that deserves to be considered.

Assembly of the supercraton Superia occurred over a protracted period that started in the late Neoarchean and continued to the early Paleoproterozoic, potentially ending at ~2.3 Ga with the Arrowsmith Orogeny in NW Canada. Associated emplacement of LIPs affected all landmasses, but their ages cluster into several discreet groups that individually are not expressed on all continents (Ernst, 2014). The initiation of the GOE, as defined by the disappearance of mass-independently fractionated sulphur (MIF-S) from sedimentary records (Holland, 2002), has been constrained between ~2.45 and 2.43 Ga (e.g., Warke et al., 2020). However, the long-term disappearance of MIF-S has been recently considered to be either globally asynchronous (Philippot et al., 2018) or to correspond to a series of rises and falls in atmospheric oxygen in association with global glaciations (Gumsley et al., 2017; Bekker et al., 2020; Poulton et al., 2021). The Paleoproterozoic glaciations are generally envisioned to have a global extent since there is strong evidence for glaciation at sea level near paleoequator (Evans et al., 1997). However, diamictites in the Boolgeeda Iron Formation (Martin, 1999) and the Koegas Subrgroup (Polteau et al., 2006), if indeed glacial, would correspond to regional-scale glaciations leading to the Snowball events. Although three stratigraphic horizons with glacial diamictites are recorded in the Huronian and Snowy Pass supergroups of Ontario and Wyoming, respectively, other Paleoproterozoic successions bear evidence for two, one, or no glaciations. Furthermore, synchronicity of Paleoproterozoic ice ages, in contrast to the Neoproterozoic glaciations, has to be tested with high-precision geochronology. Finally, the LE that was inferred to last between ~2.22 and 2.06 Ga (Karhu and Holland, 1996), might be mistaken for shorter-lived, but similar magnitude excursions leading to the LE and in its aftermath before ~2.0 Ga.

Pending future work testing synchronicity of the early Paleoproterozoic events with high-precision geochronology, it seems premature at this stage to define the GSSP based on any of these events that could be multiple and asynchronous worldwide. In contrast, the conventional approach based on the numerical value for the Archean-Proterozoic boundary avoids potential confusion and provides an independent framework to test synchronicity and global extent of the early Paleoproterozoic events.

References

Bekker, A., Krapež, B., Karhu, J.A., 2020, Correlation of the stratigraphic cover of the Pilbara and Kaapvaal cratons recording the lead up to Paleoproterozoic Icehouse and the GOE, Earth Science Reviews 211, 103389.

Evans, D.A., Beukes, N.J., Kirschvink, J.L., 1997. Low-latitude glaciation in the Paleoproterozoic era. Nature, 386: 262-266.

Ernst, R. E. (2014). Large igneous provinces. Cambridge University Press.

Gumsley, A.P., Chamberlain, K.R., Bleeker, W., Soderlund, U., Kock, M.D.O., Larsson, E.R., Bekker, A., 2017. Timing and tempo of the Great Oxidation Event. Proceedings of the National Academy of Sciences of the United States of America, 114(8): 1811-1816.

Holland, H.D., 2002. Volcanic gases, black smokers, and the Great Oxidation Event. Geochim. Cosmochim. Acta, 66(21): 3811-3826.

Karhu, J.A., Holland, H.D., 1996. Carbon isotopes and the rise of atmospheric oxygen. Geology, 24(10): 867-870.

Martin, D.M., 1999. Depositional setting and implications of Paleoproterozoic glaciomarine sedimentation in the Hamersley Province, Western Australia. Geol. Soc. Am. Bull., 111(2): 189-203.

Polteau, S., Moore, J.M., Tsikos, H., 2006. The geology and geochemistry of the Palaeoproterozoic Makganyene diamictite. Precambrian Res. 148: 257–274.

Philippot, P., Avila, J.N., Killingsworth, B.A., Tessalina, S., Baton, F., Caquineau, T., Muller, E., Pecoits, E., Cartigny, P., Lalonde, S.V., Ireland, T.R., Thomazo, C., van Kranendonk, M.J., Busigny, V., 2018. Globally asynchronous sulphur isotope signals require re-definition of the Great Oxidation Event. Nature Communications, 9.

Poulton, S.W., Bekker, A., Cumming, V.M., Zerkle, A.L., Canfield, D.E., Johnston, D.T., 2021. A 200-million-year delay in permanent atmospheric oxygenation. Nature, 592(7853): 232-236.

Warke, M.R., Di Rocco, T., Zerkle, A.L., Lepland A., Prave A.R., Martin A.P., Ueno, Y., Condon, D.J., Claire, M.W., 2020. The Great Oxidation Event preceded a Paleoproterozoic "snowball Earth". Proc. Nat. Acad. Sci. 117: 13314-13320.

Mineral identification of hydrothermal oceanic chert and banded iron formation in Archean in Pilbara terrane, western Australia

Yusuke Inokuchi [1], Shoichi Kiyokawa [2], Yuya Takeda[3] and Seiichiro Uehara [4]

1. Graduate school of Earth and Planetary science, Kyushu University, Fukuoka, Japan Inokuchi.yusuke.233@s.kyushu-u.ac.jp
2. Department of Earth and Planetary science, Kyushu University, Fukuoka, Japan kiyokawa@geo.kyushu-u.ac.jp
3. Graduate school of Integrated Science for Global Society, Kyushu University, Fukuoka, Japan
4. The Kyushu University Museum

1. Introduction

The formation of Archean BIF has been discussed, including oxidation by photosynthesis and precipitation of divalent iron by iron-reducing bacteria such as dissimilatory iron reduction (DIR) (eg. Bekker et al. 2012). However, in recent years, it has been reported that the formation of iron precipitates in Archean BIF was not accompanied by biological activity and was precipitated as greenalite ($Fe^{2+}{}_2\ Si_2\ O_5\ (OH)_4$) as a primary mineral (Rassmussen et al. al. 2013, Rasmussen et al. 2023). In this study, we conducted electron microscopy and chemical analysis of the minerals contained one of the famous Archean Iron Formation, Cleaverville Iron formation.

Within the coastal Pilbara greenstone belt in Western Australia, it has well stratified sedimentary sequence, such as in chert and BIF in the 3.2 Ga Dixon Island Formation (DX Formation) to 3.1 Ga Cleaverville Formation (CL Formation). **I**n this region has lower green schist faces metamorphism and relatively weak deformation, and the geological conditions at the time of deposition have been recorded (Kiyokawa et al. 2012).

The DX Formation consists of a komatiite-rhyolite layer, a black chert layer, and a polychrome chert layer from the bottom, and it is possible to reconstruct the hydrothermal activity with silicified volcanic rock changed to a chert layer (Kiyokawa et al. al., 2006). The CL Formation is formed black shale layer to the BIF layer remains well preserved. It was divided into the black shale layer and the BIF layer from the bottom to top. The CL Formation consist of Black shale to siderite-magnetite laminated BIF. It well preserved original sedimentary sequence of the BIF.

2. Results

In the black chert of the DX Formation pyrite was identfied together with apatite crystals (3 μm) . It identified just above brown coarbonaceos biomat layer.

The laminated chert layer of the CL Formation consists of alternating with less than 1 cm thick layers of “green clay” and “white chert” layers. As a result of XRD, the constituent minerals were siderite, quartz, and magnetite. Microscopy and SEM observations revealed that the greenish clay layer was composed of fine-grained siderite which mostly rounded particle shape (10-20 μm in diamater). The white chert layer was mainly composed of quartz and it contains later forming siderite crystals and plate-shaped chlorite crystals of about 10 to 50 μm. In addition, needle-shaped crystals of less than 5 μm were observed in the qartz matrix.

FIB-SEM observations of needle-like crystals within quartz revealed spherical iron oxide (2 μm) and needle-like crystals at grain boundaries. These needle-like crystals consist of chlorite minerals with a basal reflectance of 14 Å. STEM-EDS mapping provided the chemical composition as $(Fe^{2+}{}_{3.92},\ Al_{1.49},\ Mg_{0.64})\Sigma_{6.05}\ (Si_{2.43}Al_{1.57})\Sigma_{4.00}O_{10}(OH)_8$, identifying the mineral species as chamosite. Some quartz grains showed voids smaller than 1 μm, and needle-shaped crystals smaller than 500 nm were observed in the quartz. The crystals identified as serpentine minerals with a basal reflection of 7 Å.

The serpentine mineral’s chemical composition was determined as $(Fe^{2+}{}_{1.94},Al_{0.73},Mg_{0.28})\ \Sigma_{2.95}(Si_{1.38}Al_{0.62})\ \Sigma_{2.00}O_5(OH)_4$, and the mineral species was berchierine.

3. Discussion

The distribution and characteristics of greenalite reported in Hamersley and berchierine found in this area are similar. It suggests that berchierine may also precipitate at early stage of BIF sedimentation. Future considerations will explore where aluminum supplied from to the ocean.

References

Bekker et al. (2014) Iron formations: their origins and implications for Ancient Seawater chemistry, H.D. Holland, K.K. Turekian (Eds.), Treatise on Geochemistry (Second ed.), *Elsevier*, *Oxford*, pp. 561-628

Kiyokawa, S., et al. (2012) Lateral variations in the lithology and organic chemistry of a black shale sequence on the Mesoarchean seafloor affected by hydrothermal processes: The Dixon Island Formation of the coastal Pilbara Terrane, Western Australia. *Island Arc* **21**, 118–147.

Kiyokawa S., Ito T., Ikehara M. and Kitajima F., 2006. Middle Archean volcano-hydrothermal sequence: bacterial microfossil- bearing 3.2-Ga Dixon Island Formation, coastal Pilbara terrane, Australia. *Geological Society of America Bulletin*, vol. **118**, no. 1/2, 3-22.

Rasmussen, B., Meier, D.B., Krapeˇz, B., Muhling, J.R., (2013) Iron silicate microgranules as precursor sediments to 2.5 billion-year-old banded iron formations. *Geology* **41**, 435–438

PRE-OROGENIC RIFTING STAGE INITIATION OF THE PAN-AFRICAN OROGENY IN THE EASTERN DESERT AND SINAI, EGYPT: THE FEATURES AND EVIDENCE.

Dawoud, M.[1], El-Dokouny, H.A.[2], Mahmoud, A.S.[3] and El-Lithy, M.A.[4]

1. Geology Department, Faculty of Science, Menoufia University, Egypt dawoud_99@yahoo.com
2. Geology Department, Faculty of Science, Menoufia University, Egypt hanaaabdelnaby4@gmail.com
3. Geology Department, Faculty of Science, Fayoum University, Egypt halim.geologist@mail.ru
4. Geology Department, Faculty of Science, Menoufia University, Egypt maielleithy24@gmail.com

1. Introduction

Egyptian basement complex (EBC) is a part of the Arabian-Nubian Shield (ANS) that forms the NE section of Africa and it is regarded as an example of the East African Orogeny which was previously thought composed primarily of juvenile Neoproterozoic crust (Fritz et al., 2013) and created by numerous Neoproterozoic volcanic arcs accretion along suture zones defined by dismembered ophiolite (Patchett and Chase, 2002). EBC is exposed mainly in Sinai and the Eastern Desert (ED) comprising two units from bottom upward; i) the structural basement (Infrastructure) including high-grade metamorphic gneisses; and (ii) the structural cover (Suprastructure) including ophiolite slices, arc metavolcanics and arc metasediments (Gahlan et al. 2012). The two units were intruded by syn-tectonic calc-alkaline granites and metagabbros–diorite complex (Abd El-Wahed et al. 2010). The later stages of the crustal growth are distinguished by post-tectonic granites and Dokhan volcanics that are consistent with the deposition of molasse-type Hammamat sediments. The oldest precisely dated magmatic rocks yielded ages around 840–860 Ma (e.g. Kröner et al., 1992; Kuster et al., 2008). From this date to ~740 Ma the magmatism was predominantly oceanic: ophiolites, bimodal volcanic rocks, and immature oceanic arcs (Hargrove et al., 2006). After ~720 Ma the formed terranes began to converge and were in place. ED was subdivided by Stern and Hedge (1985) into Northern, Central and South-Eastern Desert regions (NED, CED and SED). The NED is characterized by younger rocks, such as younger granites, Dokhan volcanics and Hammamat molasse sediments, whereas older rock types rarely occur.

2. Results and discussion

It was previously known that the Northern Eastern Desert does not contain Cryogenian and Tonian igneous rocks. The most exciting recent developments in the studies of the (NED) and Sinai are the presence of small tracts of Cryogenian and Tonian igneous rocks (Stern, 2018), Tonian muscovite tonalite, I-type muscovite-bearing trondhjemite and granodiorite from W. Dara (ND) with complexity in the U-Pb zircon ages at ~ 740 Ma (Eliwa et al., 2014), the presence of ~720 Ma ignimbrites unconformably overlying the ~740 Ma granitoids (Bühler et al. 2014), the presence of ~780 Ma dacite from South Um Mongul (ND) (Abd El-Rahman et al., 2017). Moneiga quartz-diorites (South Sinai) zircon crystallization age has been precisely determined at 844± 4 Ma. About 15% of zircon contains pre-magmatic cores with ages between 1025 Ma and 1045 Ma. The initial isotope composition ($^{87}Sr/^{86}Sr_{844Ma}$ =0.703187± 0.000034; εNd_{844Ma} 3.5± 0.5) is slightly less primitive than expected and that seen in similar rocks of the Arabian-Nubian Shield with the same age. Trace-element and isotope ratios reveal the presence of a non-juvenile crustal (Bea, et al., 2009). Li et al. (2018) reported 750 Ma felsic volcanic clast from the Atud olistostrome (CED), containing a large amount (31%) of Archean-Paleoproterozoic detrital zircon with negative zircon eHf (T) values ranging from ~1.9 to ~16.3, corresponding to T_{DM}^{C} ages between 1,765 and 3,045 Ma which shows features of old continental crust reworking. Ali et al. (2010) reported (~750 Ma -790Ma) granitic clasts from the Atud diamictite in W. Kariem and W. Mobarak,(CED). The U-Pb zircon analyses exhibit minor Mesoproterozoic and more prevalent Paleoproterozoic and Neoarchean material. Besides, Wust (and Kröner, 1987) reported ~775±28 Ma granitic clasts enclosed within the Atud olistostrome in the east of Gabal Atud area. Moreover, the Atud olistostrome (east of Gabal Atud) is intruded by (~694Ma) typical island-arc metagabbro and contains abundant I-type high-K, peraluminous graphic granite, granodiorite and volcanic clasts. These igneous clasts are likely originated from magmatic activity during the pre-orogenic rift stage as well the Atud olistostrome was deposited in a pre-orogenic-rift-related basin (El-Lithy,2023).

Testing investigating and reappraisal for the available data concerning some anomalous high ages from exposed acid plutonic and volcanic rocks in the NED and Sinai in addition to clasts from the "Atud olistostrome" (CED) refer to magma generation pre-date the oceanic crust (represented in ophiolites and serpentinites) and the island arc stage in the Arabian-Nubian shield. The rifting event at ~850 Ma likely represents the best available estimate of the beginning of the prolonged breakup process of Rodinia in this region.

References

Ali, K. A., Azer, M. K., Gahlan, H. A., Wilde, S. A., Samuel, M. D., & Stern, R. J. (2010). Age constraints on the formation and emplacement of Neoproterozoic ophiolites along the Allaqi–Heiani Suture, South Eastern Desert of Egypt. *Gondwana Research*, *18*(4), 583-595.

Abd El-Rahman, Y., Seifert, T., Gutzmer, J., Said, A., Hofmann, M., Gärtner, A., & Linnemann, U. (2017). The South Um Mongul Cu-Mo-Au prospect in the Eastern Desert of Egypt: from a mid-Cryogenian continental arc to Ediacaran post-collisional appinite-high Ba-Sr monzogranite. *Ore Geology Reviews*, *80*, 250-266.

Bea, F., Abu-Anbar, M., Montero, P., Peres, P., & Talavera, C. (2009). The~ 844 Ma Moneiga quartz-diorites of the Sinai, Egypt: evidence for Andean-type arc or rift-related magmatism in the Arabian-Nubian Shield? Precambrian Research, 175(1-4), 161-168.

Bühler, B., Breitkreuz, C., Pfänder, J. A., Hofmann, M., Becker, S., Linnemann, U., & Eliwa, H. A. (2014). New insights into the

accretion of the Arabian-Nubian Shield: Depositional setting, composition and geochronology of a Mid-Cryogenian arc succession (North Eastern Desert, Egypt). Precambrian Research, 243, 149-167.

El-Lithy, M.A., 2023. Diamictites from the Eastern Desert of Egypt: Implications for the Paleo-geological Processes and Paleo-climatology. PhD Thesis, Menoufia University.

Eliwa, H. A., Breitkreuz, C., Murata, M., Khalaf, I. M., Bühler, B., Itaya, T., ... & El Gameel, K. (2014). SIMS zircon U–Pb and mica K–Ar geochronology, and Sr–Nd isotope geochemistry of Neoproterozoic granitoids and their bearing on the evolution of the north Eastern Desert, Egypt. Gondwana Research, 25(4), 1570-1598.

Fritz, H., Abdelsalam, M., Ali, K. A., Bingen, B., Collins, A. S., Fowler, A. R., ... & Viola, G. (2013). Orogen styles in the East African Orogen: a review of the Neoproterozoic to Cambrian tectonic evolution. *Journal of African Earth Sciences*, *86, 65-106.*

Li, X. H., Abd El-Rahman, Y., Abu Anbar, M., Li, J., Ling, X.X., Wu, L. G., and Masoud, A.E. (2018). Old continental crust underlying juvenile oceanic arc: Evidence from Northern Arabian-Nubian Shield, Egypt. *Geophysical Res. Letters, 45(7), 3001–3008. https://doi.org/10.1002/2018GL077121.*

Stern, R. J. (2018). Neoproterozoic formation and evolution of Eastern Desert continental crust–The importance of the infrastructure-superstructure transition. *Journal of African Earth Sciences*, *146*, *15-27.*

Wust, H.J., Todt, W., and Kröner, A., (1987). Conventional and single grain zircon ages for metasediments and granite clasts from the Eastern Desert of Egypt: Evidence for active continental margin evolution. In: Pan-African times. Terra Cognita, 7: 333-334.

DISTURBANCE OF ISOTOPIC RATIOS, U-Pb SYSTEMATICS AND TRACE ELEMENTS DURING THE ALTERATION OF ZIRCON: IMPLICATIONS FROM THE YOUNGER GRANITES OF EGYPT.

Dawoud, M. , [*,1] Orihashi, Y.,[2] El-Dokouny, H.A.,[3] Mahmoud, A.Sh.,[4] El-Lithy, M.A.,[5] Shebl, A.,[6] and Abdelkader, M.A.,[7,8]

1 Geology Department, Faculty of Science, Menoufia University, Egypt
dawoud_99@yahoo.com * Corresponding author
2 Department of Earth and Environmental Sciences, Hirosaki University, Japan
oripachi@hirosaki-u.ac.jp
3 Geology Department, Faculty of Science, Menoufia University, Egypt
hanaaabdelnaby4@gmail.com
4 Department of geology, University of Fayoum, Al-Fayoum, Egypt
asm07@fayoum.edu.eg
5 Geology Department, Faculty of Science, Menoufia University, Egypt
maielleithy24@gmail.com
6 Department of Mineralogy and Geology, University of Debrecen, Hungary
ali.shebl@science.tanta.edu.eg
7,8 Department of Earth Resource Science, Akita University, Japan
Department of Geology, Faculty of Science, Menoufia University, Egypt
mohammed.ali19924487@gmail.com

1. Introduction:

The pan-African basement rocks of Egypt are exposed in the Eastern Desert and south Sinai. The involved granitoids are traditionally and simply classified into the older (or grey granitoids around 660 ma) granitoids and the younger (or buff, pink or red granites around 630 ma) granites; Akaad and El Ramly 1960. The studying of zircons (abundance, typology, morphology, internal structures, overgrowths, inclusions, inheritance, chemistry, isotopes and ages) has contributed considerably in revealing and solving many problems from those granitoids; Kabesh et al., 1999, Gharib and Dawoud 2005. In general zircon is known as resistant and robust mineral, however, zircon could be altered (other than metamictization) by magmatic or later fluids reactions. The alteration of zircon is recorded and utilized for some aspects as the nature and origin of the invading fluids, Geisler et al., 2003, Dawoud 2004 and the ore genesis, Zhai et al., 2022 and references therein.

In this work we introduce new data using LA-ICP-MS for trace elements, isotopic ratios and U-Pb ages in altered and fresh zircons from some younger (Gattarian) granites, North Eastern Desert, Egypt. It is a trial to understand the effect of those hydrothermal fluids or solutions on the composition the zircons, their isotopic ratios and ages.

2- Results and discussion:

Zircons from the studied youner granites are characterized by the dominance of the prism {100} and the pyramid {101}. Most of those zircons are not so clear but could be turbid with reddish tint. The petrographical investigations indicate that the zircons are selectively altered according to the possibility if the grain can be reached by the hydrothermal solutions through the available pathways or the resistance or protection of the enclosing mineral towards those solutions.

The back scattered electron images (rather than the cathodoluminescence) are very effective to reveal and distinguish between the fresh and altered spots. Although the alteration enriches the infected spots with the heavier atoms (e,g. U, Y and HREEs) those altered spots are darker which could refers to the transformation in the crystallization and physical state into the amorphous material.

From the chemical point of view almost all the analysed trace elements are affected during the alteration process either by enrichment or depletion. The most important and drastic impact is the increment of the U, Th, Pb and HRREs in the altered patches. On the other side; the isotopic ratios $^{238}U/^{206}Pb$ are greatly disturbed, affected and decreased due to the alteration consequently the ages diminished. The estimated ages for the fresh spots are around 640 ma which is the crystallization age, while the ages from the altered spots are varied and decrease down to 268 ma. The results and outcomes of this study emphasize the cautions that have to be considered during the dealing and selecting the zircon grains for dating, the isotopic ratios and ages from such altered zircons.

References:

Akaad, M,K., El-Ramly, M.F., (1960). Geological history and classification of the basement rocks of the central Eastern Desert of Egypt. Geol. Surv. Egypt. Paper No 9, 24 pp

Dawoud, M., (2004). The nature and origin of U-bearing fluids as revealed from zircon alteration: examples from the Gattarian granites of Egypt. Sixth International Conference of Geochemistry, Alexandria University, I-B, 875-891.

Geisler;T., Rashwan, A. A., Rahn, M. K. W., Poller, U., Zwingmann, H., Pidgeon, R. T., Schleicher, H., and Tomaschek, F., (2003). Low-temperature hydrothermal alteration of natural metamict zircons from the Eastern Desert, Egypt. Mineralogical Magazine, June 2003, Vol. 67(3), pp. 485–508.

Gharib,M.E., and Dawoud,M., (2005). Inheritance in zircon from Aswan granitoids: the role of contamination at the western boundary of the Nubian shield. 1st Inter. Conf. Geol. Tethys, Cairo Univ., p. 11-28.

Kabesh, M.L., Atia, M.S., .and Dawoud, M., (1999). Typology and microprobe analysis of zircons as an indicator to evolution and genesis of Abu El Hasan granitoids, Northern Eastern Desert, Egypt. Acta. Min-Petrog., Szeged, XL, 21-44

Zhai, W., Zhang, E., Zheng, Si., Santosh, M., Sun, X., Niu, H., Fu, B., Fu, Y., Li, D., Jiang,Y., Liang,F., Lin,W., Zhao, Y., and Han, S., (2022). Hydrothermal zircon: Characteristics, genesis and metallogenic implications, Ore Geol. Rev.. V. 149, 105111.

DISTINGUISHING BETWEEN OROGENIC AND INTRUSION-RELATED GOLD MINERALIZATIONS: AN EXAMPLE FROM THE ABU GAHARISH PROSPECT IN EGYPT

Abdelhalim Mahmoud [1], Hanaa El-Dokouny [2], Mohamed Ghoneim [3], Mai El-Lithy [2], Viktor Dyakonov [4], Ilya Vikent'ev [5], Arizh Dolomanova-Topol [5], Maher Dawoud [2]

1. Department of geology, University of Fayoum, Al-Fayoum, Egypt
   asm07@fayoum.edu.eg
2. Department of geology, University of Menofia, Shebin ElKoum, Egypt
   hanaaabdelnaby4@gmail.com, maielleithy24@gmail.com & dawoud_99@yahoo.com
3. Department of Geochemical Exploration, Nuclear Materials Authority, Cairo, Egypt
   moh.gho@mail.ru
4. Department of general geology, Russian State Geological Prospecting University, Moscow, Russia
   Mdf.rudn@mail.ru
5. Laboratory of geology of ore deposits, Institute of Geology of Ore Deposits, Petrography, Mineralogy and Geochemistry, the Russian Academy of Sciences (IGEM RAS), Moscow, Russia
   vikentevilya@gmail.com & arij_belochka@mail.ru

1. Introduction

The Abu Gaharish is a small, granitic body of nearly oval shape. Mineralizations were detected as high-grade quartz veins along the entire eastern boundary of the Gaharish granitic body over a strike distance of more than 5 km. The occurrence of wolframite hosted in some portions of the pluton may refer to its belonging to reduced intrusion-related gold (RIRG) deposits.

2. Results

The auriferous quartz veins of the Abu Gaharish prospect are and are hosted in an NNE-trending shear zone along the contact between the Abu Gaharish Younger granites and a volcano-sedimentary succession. These veins experienced successive stages of shearing, deformation, and recrystallization, mainly bulging recrystallization (BLG) textures indicating a low temperature of formation between 250 and 400 °C (e.g., Gibert et al., 1998).

The low contents of granitophile elements (such as Mo, Sn, and W) in the quartz veins at Abu Gaharish indicate that the gold-sulfide-quartz veins have no linkage with granitoid intrusion. However, enrichment of these elements in the inner alteration zone is attributed to their leaching by hydrothermal fluids from anomalous zones.

The EPMA results indicate a high Co:Ni ratio of pyrites, giving evidence for their formation under low-temperature magmatic-hydrothermal conditions (e.g., Xuexin 1984). Also, the lack of Bi and Sb and the low Ag content in the galena give indications for their formation in decreasing temperature conditions (e.g., Fleischer 1956).

Fluid inclusion studies indicate that the ores of the Abu-Gaharish deposit were formed under a temperature range of 355-232 °C from low-salinity fluids predominantly composed of Mg, (Na, K,)-chlorides with salt concentrations ranging from 5.2 to 1.7 wt % equiv. NaCl with some CO_2 and little methane. This salinity and homogenization temperature (T_h) are equivalent to orogenic gold deposits with no indication of magmatic or meteoric contamination, based on the diagram of Roedder (1984), modified after Wilkinson (2001). The ore-forming fluids of the Abu Gaharish prospect appear to have originated from devolatilization of metamorphic sources (Kesler 2005), where leaching of S, Au, and Ag from volcano-sedimentary rocks occurred under greenschist-amphibolite facies regional metamorphism.

3. Discussion

The geological characteristics of Abu Gaharish mineralizations, which include not-sheeted epigenetic quartz veins formed later than the hosting granitoids related to structurally controlled shear zones, metamorphic terrains, low sulfide content, and post-peak metamorphic setting, are comparable to those of orogenic deposits. On the other hand, the lack of tellurides, molybdenite, cassiterite, wolframite, rutile, ilmenite, and Bi-rich galena, our fluid inclusion data, as well as the volcanic arc tectonic setting of the Abu Gaharish granitoids, do not support any intrusion-related linkage with Abu Gaharish granitoids.

References

Fleischer, M. (1956), Minor Elements in Some Sulfide Minerals?, *Economic Geology*, 50th Anniversary Volume, p. 970–1024.

Gibert, F., M.-L. Pascal, and M. Pichavant (1998), Gold solubility and speciation in hydrothermal solutions: Experimental study of the stability of hydrosulphide complex of gold (AuHS) at 350 to 450 C and 500 bars, *Geochimica et Cosmochimica Acta*, **62**(17), 2931-2947

Kesler, S. E. (2005), Ore-forming fluids, Elements, **1**(1), 13-18.

Roedder, E. (1984), Volume 12: fluid inclusions, *Reviews in mineralogy*, **12**, 644.

Wilkinson, J. (2001), Fluid inclusions in hydrothermal ore deposits, Lithos, **55**(1-4), 229-272.

Xuexin, S. (1984), Minor elements and ore genesis of the Fankou lead-zinc deposit, China, *Mineralium Deposita*, **19**, 95-104.

THE GEOLOGY OF GOLD MINERALIZATION IN THE NANGODI GREENSTONE BELT, NE GHANA

Kwame Fynn[1], Axel Hofmann[1], and Samuel Nunoo[2]

1. Department of Geology, University of Johannesburg, Johannesburg, South Africa kfynn@uj.ac.za, ahofmann@uj.ac.za
2. Department of Earth Science, University of Ghana, Accra, Ghana snunoo@ug.edu.gh

1. Introduction

The Birimian of the West African Craton comprises a Palaeoproterozoic granitoid-greenstone terrain (Abouchami et al., 1990; Sylvester & Attoh, 1992). Among the greenstone belts is the NE-SW trending Bole-Nangodi belt located in the northern part of Ghana (Attoh, 1982). It consists of volcanic and volcaniclastic rocks (basalt to rhyolite) and immature sedimentary rocks (greywacke, shale), and is flanked on both sides by extensive granitoid complexes (Attoh, 1982; de Kock et al., 2012; Block et al., 2016). These rocks have been affected by the 2.1 Ga Eburnean orogeny, which deformed and metamorphosed the rocks under greenschist facies conditions, accompanied by gold mineralization (Milési et al., 1992).

2. Results

Until the recent gold deposit discovery by Cardinal Resources (Namdini Gold Project) in the Nangodi belt (Tomlinson et al., 2020), very little attention had been given to the rocks in the belt and the associated gold mineralization. This study presents U-Pb zircon ages, (ore) petrographic observations, and whole rock major and trace element data from outcrop and drill core samples (including drill cores from the Namdini Gold Project).

3. Discussion

The rocks are predominantly arc-related metavolcanics of basaltic to rhyolitic composition that are deformed to variable degrees and altered by CO_2-rich hydrothermal fluids. Hydrothermal gold mineralization is associated with disseminated sulphides that occur with quartz-carbonate veins and are usually restricted to high-strain zones in the metavolcanics. Compositional zoning in the sulphides implies changes in the chemistry of metal-transporting fluids. Zircon ages indicate that the volcanic units were deposited at ca. 2.16 Ga, followed by syn- and post-tectonic granitic intrusions at ca. 2.12 Ga and 2.10 Ga, respectively. The presence of sulphides in the metavolcanics and the syn-tectonic granite, in contrast to their absence in the post-tectonic granite, suggests a syn- to late-tectonic mineralization that ended before 2.10 Ga.

References

Abouchami, W., Boher, M., Michard, A., & Albarede, F. (1990). A major 2.1 Ga event of mafic magmatism in West Africa: an early stage of crustal accretion. Journal of Geophysical Research: Solid Earth, 95, 17605-17629.

Attoh, K. (1982). Structure, gravity models and stratigraphy of an early Proterozoic volcanic—sedimentary belt in northeastern Ghana. Precambrian Research, 18, 275-290.

Block, S., Ganne, J., Baratoux, L., Zeh, A., Parra‐Avila, L. A., Jessell, M. & Siebenaller, L. (2015). Petrological and geochronological constraints on lower crust exhumation during Paleoproterozoic (Eburnean) orogeny, NW Ghana, West African Craton. Journal of Metamorphic Geology, 33, 463-494.

De Kock, G. S., Théveniaut, H., Botha, P. M. W., & Gyapong, W. (2012). Timing the structural events in the Palaeoproterozoic Bolé–Nangodi belt terrane and adjacent Maluwe basin, West African craton, in central-west Ghana. Journal of African Earth Sciences, 65, 1-24.

Milési, J. P., Ledru, P., Feybesse, J. L., Dommanget, A., & Marcoux, E. (1992). Early Proterozoic ore deposits and tectonics of the Birimian orogenic belt, West Africa. Precambrian Research, 58, 305-344.

Sylvester, P. J., & Attoh, K. (1992). Lithostratigraphy and composition of 2.1 Ga greenstone belts of the West African Craton and their bearing on crustal evolution and the Archean-Proterozoic boundary. The Journal of Geology, 100, 377-393.

Tomlinson, K., Abbott, P., Opoku-Boamah, E., Owusu-Ansah, E., Affi, S., Bray, R., & Taylor, E. (2020). Namdini Gold Deposit, Upper East Region, Ghana—One of the Largest West African Gold Discovery in a Decade (p. 16). Cardinal Resources Limited.

Lithology and Stratigraphy of Paleoproterozoic Volcaniclastic Sequences in the Cape Three Points area of the Ashanti Birimian Greenstone Belt in Ghana.

Satoshi Yoshimaru[1], Shoichi Kiyokawa[1], Takashi Ito[2], Kenji Horie[3], Mami Takehara[3], Kwabina Ibrahim[4], George M. Tetteh[4], and Frank K. Nyame[5]

1. Department of Earth and Planetary Sciences, Kyushu University, Fukuoka, Japan (Yoshimaru.satoshi.536@s.kyushu-u.ac.jp)
2. Ibaraki University, Mito, Japan.
3. National Institute of Polar Research, Tokyo, Japan.
4. University of Ghana, Legon, Ghana.
5. University of Mines and Technology, Tarkwa, Ghana.

1. Introduction

A Paleoproterozoic greenstone terrane of Ghana, the Ashanti belt has been worked on to establish a new geologic site and stratigraphy for future research of the earth's history during the Great Oxidation Event.

The Ashanti belt is a NE-SW trending terrain in southwest Ghana. Components of it, at the southern part, are dominantly the Lower Birimian series of metavolcanics/ volcaniclastics and granitoids (Loh et al., 1999). The Lower Birimian rock series in the area forms three greenstone branches including the Cape Three Points branch which is the focus. It is constrained by the zircon U-Pb age of a juxtaposed granitoid body at 2.17 Ga (Hirdes et al., 1992).

2. Study Area

Study area of this research, in the Cape Three Points branch, is within the coastline extending west to east for about 4 km, between Kutike cape and Akodaa village. The area outcrops well-preserved bedded metasedimentary rocks originated from volcanic activities and some intrusions. The area was divided usings tructural discontinuities into four sections from west to east: Kutike (Ku), Atwepo West (At-W), Atwepo East (At-E), and Akodaa (Ak).

3. Geological Structure

Ductile deformations were observed at the western margin of Ku section and at the western side of At-E section. The latter is not continuous to the At-W section across the sectional boundary. There is a brittle crush zone of a porphyry intrusion at the sectional boundary due to a fault which separates these sections. Between the Ku and At-W sections and the At-E and Ak sections, there are relatively intense brittle deformations related within the fault zone. These could cause some stratigraphic discontinuities yet the bedded metasedimentary rocks keep their original stratigraphic sequence within each section not withstanding small gaps in outcrop exposure and brittle faults.

4. Lithology

Main formations in the study area are volcanic and metavolcaniclastic rocks. These show facies variety of turbidites, argillite/chert, massive deposits, and lavas. The most dominant facies are turbidites in all the sections. Bed thickness is normally less than 1 m, and composed of volcanic ash and lapilli, occasionally including lithic fragments and rip-up (mud) crusts. Turbidite beds tend to be massive at the base and parallel or cross laminated at the middle to the top, and graded. The turbidite facies are often associated with argillite/chert facies which are composed of calc-siliceous and mafic micritic grains forming white to pale green layers. The argillite facies are usually less than 20 cm in thickness in wide areas of the Ku section, At-W section, and Ak section, and in small areas of the At-E section. The massive facies show thickness of single beds more than 5 m, with graded bedding at the top. They tend to contain larger breccia fragments, lithic fragments, welded texture, and accretionary lapilli. They occur in the middle of a coarsening upward sequence of the Ku section and At-E section and at the base of a fining upward sequence of the Ak section. The lava facies are unique for the At-E section. They were affected by ductile deformation partially, but still preserve pillow shaped and sheeted lavas within the 200 m thick stratigraphic pile intercalated with turbidite facies.

5. Depositional Age

Age data were obtained by zircon U-Pb method with SHRIMP at the National Institute of Polar Research. From the At-E section, a quartz-hornblende porphyry dike gave 2265.6±4.6 Ma (n=48, MSWD=0.95), which constraints the minimum depositional age of the wall rocks of metasedimentary rocks. From the Ak section, a massive volcaniclastic bed gave 2172.6±-8.8 Ma (n=35, MSWD=1.07), which constrains the maximum depositional age of this bed.

6. Stratigraphy

Each structural section forms a particular stratigraphic unit. Ku unit (~400m) and At-W unit (~600m) were similar because they are dominated by turbidite facies and argillite facies beds. At-E unit (~900m) displays a significant volume of massive deposition facies and lava facies intercalated with a smaller amount of turbidite facies and argillite facies. Ak unit (~200m) is composed mainly of argillite facies, accompanied with minor turbidite facies and massive deposited facies.

These units were dominated by volcanic materials such as ash, lapilli, breccias, and lavas, therefore they must have originated from single/multiple volcano(es) and recorded its evolution at each setting and timing respectively for each stratigraphic unit. The depositional facies seem to reflect the magnitude of the eruptions and/or the vertical and lateral distance from the source volcano(es).

References

Hirdes et al. (1992) Reassessment of Proterozoic granitoid ages in Ghana on the basis of U/Pb zircon and monazite dating. Precambrian Research 56, 89-96.

Loh, G. et al. (1999) Explanatory Notes for the Geological Map of southwest Ghana 1:100,000 Sekondi (0402A) and Axim (0403B) Sheets. Hannover

OCEAN REDOX FLUCTUATION DURING THE EARLY PALEOPROTEROZOIC

Kento Motomura[1], Andrey Bekker[1], and Chadlin M. Ostrander[2]

1. Department of Earth and Planetary Sciences, University of California, Riverside, USA
2. Department of Geology and Geophysics, University of Utah, Salt Lake City, USA

1. Introduction

The Great Oxidation Episode (GOE) and Lomagundi Event (LE), which are dated at *ca.* 2.43 Ga and 2.2-2.06 Ga, respectively, were the first, largest environmental transition (Bekker, 2022b; Bekker, 2022a). During this period, Earth's atmosphere was oxidized up to approximately 10^{-2} of the present atmospheric level, as suggested by disappearance of mass-independent sulfur isotope fractionation (Farquhar et al., 2007). Some studies, furthermore, suggested that eukaryotes have appeared soon after the GOE (e.g., Ossa Ossa et al., 2023). However, evolution of ocean environments including nitrogen bioavailability and redox state remains controversial.

Here we examine local nitrogen bioavailability and carbon cycling during the early Paleoproterozoic, with determination of organic carbon and nitrogen isotope composition for the *ca.* 2.1 Ga Uvé and Hautes Chutes formations of the Labrador Trough, eastern Canada. Redox-sensitive element and Tl isotope analysis were performed for black shales of the Hautes Chutes Formation, along with the carbon and nitrogen isotope study, to estimate global redox conditions. The Uvé and Hautes Chutes formations consist of dolomite and black shales, respectively, which could represent transgression of the ocean (Clark and Wares, 2005).

2. Results and Discussion

Dolomites of the Uvé Formation possess positive carbonate carbon isotope composition, which is consistent with deposition during LE. The average organic carbon and nitrogen isotope values of the dolomites are −25‰ and +6.3‰, respectively. Organic carbon isotope values of the dolomites show a gradual decrease down to approximately −30‰, with an increase of isotope fractionation between carbonate and organic carbon ($\Delta_{carb-org}$). Organic carbon and nitrogen isotope values of black shales of the Hautes Chutes Formation are approximately −40‰ and +5.3‰, respectively. Those variations in isotope values across the boundary between the Uvé and Hautes Chutes formations could have resulted from redox stratification. $\Delta_{carb-org}$ values of the Uvé Formation are identical to that caused by photoautotrophs using the reductive pentose phosphate cycle (Calvin cycle) to assimilate carbon (Schidlowski, 2001). More negative carbon isotope values of the Hautes Chutes Formation represent contribution of biomass using the reductive acetyl-CoA pathway (Wood-Ljungdahl pathway) and/or enhanced methane cycling in an euxinic zone (Karhu and Bekker, 2020). Nitrogen cycling was aerobic, as suggested by positive nitrogen isotope values throughout the study section, which is consistent with oxygenated surface oceans after the GOE (Kipp et al., 2018).

V/TOC, U/TOC, and Mo/TOC ratios are significantly low, suggestive of drawdown of redox-sensitive element concentration during the LE (Asael et al., 2018). Low Tl isotope values of approximately −4‰ are observed at the upper Hautes Chutes Formation. The low values could indicate Mn-oxide burial in the early Proterozoic ocean.

References

Asael, D., Rouxel, O., Poulton, S.W., Lyons, T.W., Bekker, A., 2018. Molybdenum record from black shales indicates oscillating atmospheric oxygen levels in the early Paleoproterozoic. *American J. Sci.* **318**, 275–299.

Bekker, A., 2022a. Great Oxidation Event, *Encyclopedia of Astrobiology*, pp. 1–9.

Bekker, A., 2022b. Lomagundi Carbon Isotope Excursion, *Encyclopedia of Astrobiology*, pp. 1–7.

Clark, T., Wares, R., 2005. Lithotectonic and Metallogenic Synthesis of the New Québec Orogen (Labrador Trough).

Farquhar, J. et al., 2007. Isotopic evidence for Mesoarchaean anoxia and changing atmospheric sulphur chemistry. *Nature* **449**, 706–709.

Karhu, J.A., Bekker, A., 2020. Carbon Isotopes in the Solar System, *Encyclopedia of Astrobiology*, pp. 1–10.

Kipp, M.A., Stüeken, E.E., Yun, M., Bekker, A., Buick, R., 2018. Pervasive aerobic nitrogen cycling in the surface ocean across the Paleoproterozoic Era. *Earth Planet. Sci. Lett.* **500**, 117–126.

Ossa Ossa, F. et al., 2023. Zinc enrichment and isotopic fractionation in a marine habitat of the c. 2.1 Ga Francevillian Group: A signature of zinc utilization by eukaryotes? *Earth Planet. Sci. Lett.* **611**, 118147.

Schidlowski, M., 2001. Carbon isotopes as biogeochemical recorders of life over 3.8 Ga of Earth history: evolution of a concept. *Precambrian Res.* **106**, 117–134.

The restoration of sedimentary environment of Mudstone sequences in Goto Group, Nagasaki Prefecture, Japan

Hiroaki Takahashi[1], Shoichi Kiyokawa[1], Masaru Yasunaga[2], Yuta Ikebata[3], Naoto Takahata[4]

1. Kyushu university
2. TOKYO SOIL RESEARCH CO., LTD.
3. Dia Nippon Engineering Consultants Co., Ltd.
4. The University of Tokyo, AORI

1. Introduction

The Goto Islands are located at the westernmost part of the Japan and consist of the lower to middle Miocene deposition which associated with the Japan Sea expansion. The Goto Group was deposited around 22-15 Ma and is 2000-3000 m thick, consisting of volcaniclastic rocks in the lower unit, small-scale river and lake sediments in the middle unit, and thick river sediments in the upper unit (Kiyokawa et al., 2022). To clarify the deposited environmental conditions of the stratigraphic units of the Goto Group, we focused on mudstones containing organic matter and conducted sedimentary layer analysis in detailed outcrops and microscopic observation of fresh mudstones. Total organic carbon (TOC) analysis, carbon isotope ratio ($\delta^{13}C_{org}$), total sulfur (TS), and sulfur isotope ratio ($\delta^{34}S$) measurements were conducted to investigate the origin state of organic matter and the contribution of sulfate-reducing bacteria.

We focused on the black mudstone containing organic matter in the lower to the upper part of the Goto group. Thin sections of these rocks were prepared and the characteristics of the constituent minerals and organic matter was observed using optical and electron microscopes. TOC and $\delta^{13}C_{org}$ of 112 bulk mudstone samples were measured at the Kochi Core Center using an elemental analyzer FlashEA1112 (Thermo Electron Corporation) after drying and grinding the samples and removing carbonate using 6NHCl. TS and $\delta^{34}S$ of 30 bulk samples were measured using a stable isotope ratio analyzer (Isoprime 100) at the Atmosphere and Ocean Research Institute, The University of Tokyo. Finally, elemental analysis of mudstones with carbonate particles was performed using EPMA in Kyushu University.

2. Results

The lower part of the upper unit (Toyanokubi) consists of sandstone-mudstone alternation with big ε -type cross bedding and is formed over 10 m thickness. The upper part of the unit can be traced for several hundred meters on the lateral side between the upper fine-grained mudstone layers, which are several 10 cm to 1 m thick. The sandstone is interbedded with charcoal and silicified wood several centimeters thick with well-developed parallel lamination. The depositional environment is a floodplain around the periphery of a large river. Within most mudstone contains silt-sized quartz and plant fragments. Seven samples' data were shown as TOC ranged from 0.32 to 0.62 %, $\delta^{13}C_{org}$ ranged from -32.8 to 25.0‰. Most samples are no TS amount, only two samples show 0.10 %. The TOC and $\delta^{13}C_{org}$ of charcoal (lignite) were 5.80% and -25.4%, respectively. Uniquely, the mudstone sample, which is no side changes, contains carbonate particles with brown oval shells of 30 μm in size. $\delta^{13}C_{org}$ is lighter than -30‰.

Analyzing this mudstone in EPMA, the inner of these shells is considered to be a chlorite composed of $(Mg,Fe,Al)_6(Al,Si)_4O_{10}(OH)_8$. The outer is few rich in Fe, Mg, Al.

3. Discussion

Land plants can be divided into C_3 (ex. beech) and C_4 plants(ex.cactus) based on differences in their photosynthetic circuits through free exchange of atmospheric CO_2 (Vander Merwe, 1982:Cormie and Schwarcz, 1994). The $\delta^{13}C$ of C_3 plants, which prefer low temperature and humid environments, ranges from -21 to -35‰, while C_4 plants, which prefer relatively warm and dry environments, is higher, ranging from -6‰ to -19‰. Carbon isotope ratios in the mudstones of the Goto Group range from -32.8 to -23.9‰, suggesting that the mudstones are derived from C_3 plants.

The total sulfur content is less than 0.3% in 29 samples, and the TOC/TS ratio (Berner and Raiswell, 1984) also indicates a freshwater nature. The mudstones in this area show a freshwater depositional environment without the influence of seawater, supporting the facies analysis that the Goto Group is origins of river or lake.

4. Conclusion

The average TOC and $\delta^{13}C_{org}$ of the mudstone layers of the Goto Group are 0.2% and -25.4‰, respectively. These values are consistent with those of charcoal measured by itself and are thought to originate from C_3 plants such as pine-sider trees that were growing in the area at that time. Even very low sulfur water condition, there is a possibility that there were euxinic water condition with activities such as sulfate-reducing bacteria at oxbow lake condition within food plane.

References

Kiyokawa, S. et al, 2022, Stratigraphic reconstruction of the lower-middle Miocene Goto Group, Nagasaki Prefecture. Japan, Islands arc, p.1-39. https://doi.org/10.1111/iar.12456

Cormie, A. B. and Schwarcz, H. P., 1994: Stable isotopes of nitrogen and carbon of North American White-tailed deer and implications for paleodietary and other food studies. Palaeogeography, Palaeoclimatology, Palaeoecology, 107, 227-241.

Berner, R. A. and Raiswell, R., 1984, C/S method for distinguishing freshwater from marine sedimentary rocks. Geology, 12, 365-368

PLIO-PLEISTOCENE CONTINENTAL CARBONATES AND SILCRETES IN WADI EL-NATRUN, NW EGYPT: THEIR MORPHOLOGY AND PALEOENVIRONMENTAL SIGNIFICANCE

H.A. Wanas[1], L.H. Tanner[2], M.M. Khalifa[3], F.A. Mousa[3]

1. Department of Petroleum Geology and Sedimentology, Faculty of Earth Science, King Abdulaziz University, Jeddah, Saudi Arabia
2. Department of Biological & Environmental Sciences, Le Moyne College, Syracuse, NY, 13214, USA
3. Department of Geology, Faculty of Sciences, Menoufia University, Egypt

Email: fatma.abdelgalil1@gmail.com

1. Introduction

Continental carbonates and silcretes attract the attention of sedimentologists due to their paleoclimatic and paleoenvironmental significance (Alonso-Zarza and Wright, 2010; Bustillo, 2010; Tanner, 2010). Although there have been previous studies of continental carbonates in Egypt (Khalaf and Gaber, 2008), the formations studied herein (especially calcretes, palustrine carbonates, dolocretes and silcretes) have not been investigated in detail previously. Therefore, the present work aims to deduce the paleoenvironmental conditions that prevailed during the deposition of Quaternary continental carbonates hosted within the Plio-Pleistocene sequence (Meikheimin and Qataji formations) in the southwest of Wadi El-Natrun. This is achieved through detailed field observation augmented by petrographic, mineralogical and stable isotopes.

2. Results

The lower Pliocene Meikheimin Formation display a calcrete-silicified calcrete profile. It is composed of calcareous and siliceous quartz arenite and sandy and siliceous lime-mudstone microfacies. Silcretes exhibits well-developed phases of silica cement. The Pliocene-Pleistocene Qataji Formation is composed of pink to buff-colored limestones that lack marine fossils and exhibit pisolitic, oncoidal, stromatolitic, nodular, and brecciated appearance. The microfacies include lime-mudstone, packstone and calcrete and dolocrete bearing microfacies. The microfacies exhibit micro-morphological features including nodulation, circum-granular and planar cracks, clotted fabrics, peloidal textures, infilling of burrows, root molds, pseudosparitic and microsparitic textures and fenestral pores. The Meikheimin Formation display negative $\delta^{13}C$ values that range from - 8.4 to - 7.4‰ (VPDB). The $\delta^{18}O$ values range from - 7.7‰ to - 6.9‰ (VPDB). The carbonate samples of the Qataji Formation display negative $\delta^{13}C$ values that range from - 11.1 to - 1.1‰ (VPDB). The $\delta^{18}O$ values range from -6.0‰ to +4‰ (VPDB). X-ray diffraction analysis of the studied carbonates showed the predominance of low-Mg calcite, dolomite and quartz. SEM examination revealed occurrence of bundles of fibrous palygorskite.

3. Discussion

To deduce the prevailing paleoenvironmental conditions during the deposition of the Plio-Pleistocene continental carbonate sequence at Wadi El-Natrun, we examined and compared the macro- and micro-morphological, mineralogical and stable isotopic characteristics of calcretes, dolocretes, palustrine carbonates, and silcretes of the Meikheimin and Qataji formations. Calcrete were developed in mixed vadose and phreatic diagenetic environments under an arid to semi-arid climate. Palustrine carbonates of the Qataji Formation developed as nodular, desiccated, brecciated, mottled and pisoidal limestones that are interbedded with the calcretes. They exhibit varied micro-morphological features, which indicate modifications during subaerial exposure. The dolocrete facies in the Qataji Formation includes spheroidal dolomite and dolomicrite with Mg-rich clays that formed as primary precipitates in a continental setting. The silcretes consist of spheroidal, and opaline accumulations that formed as replacements of calcrete and dolocrete. These features reflect silicification in near-surface environments where there was an interplay between vadose and phreatic environments during deposition and early burial diagenesis. The stable isotopic data suggest deposition under warm, seasonally arid to semi-arid climatic conditions in an area dominated by C3 vegetation. The regional water table was higher in the early Pleistocene than during the early Pliocene but was subject to large fluctuations.

References

Alonso-Zarza, A.M., Wright, V.P., 2010. Calcretes. In: Alonso-Zarza, A.M., Tanner, L.H. (Eds.), Carbonates in Continental Settings: Facies, Environment, and Processes. Developments in Sedimentology, vol. 61, pp. 225–267.

Bustillo, M.A., 2010. Silicification of continental carbonates. In: Alonso-Zarza, A.M., Tanner, L.H. (Eds.), Carbonates in Continental Settings: Geochemistry, Diagenesis and Applications: Developments in Sedimentology 62. Elsevier, Amsterdam, pp. 153–178.

Khalaf, F.I., Gaber, A., 2008. Occurrence of cyclic palustrine and calcrete deposits within the Lower Pliocene Hagul Formation, East Cairo district, Egypt. J. Afr. Earth Sci. 51, 298–312.

Tanner, L.H., 2010. Continental carbonates as indicators of paleoclimate. In: Alonso- Zarza, A.M., Tanner, L.H. (Eds.), Int. Assoc. Sedimentol. Spl. Publ.: Facies. Environ. Process. Dev. Sedimentol. 62, 179–214.

Impact of the Agulhas Return Current on the oceanography of the Indian sector of the Southern Ocean during late Quaternary

Minoru Ikehara[1], Matthieu Civel-Mazens[2] and Xavier Crosta[3]

1. Marine Core Research Institute (MaCRI), Kochi University, Kochi, Japan
   ikehara@kochi-u.ac.jp
2. Laboratoire des Sciences de L'Environment Marin (LEMAR), Brest, France
3. UMR CNRS 5805 EPOC, Université de Bordeaux, France

1. Introduction

The Atlantic Meridional Overturning Circulation (AMOC) plays a central role in climate through its heat and freshwater transports. The Atlantic Ocean receives warm, saline water from the Indo-Pacific Ocean through Agulhas leakage around the southern tip of Africa. Recent findings suggest that Agulhas leakage is a crucial component of the climate system and that ongoing increases in leakage under anthropogenic warming could strengthen the AMOC at a time when warming and accelerated meltwater input in the North Atlantic. The Agulhas leakage is controlled by the position of the maximum Southern Hemisphere westerly winds. These winds are related to the latitude of the oceanic subtropical front (STF), which separates the subtropical gyre from the Antarctic Circumpolar Current (ACC). If the westerlies shift northwards during the glacial climate, the oceanic "gateway" between the African continent and the STF narrows and leakage from the Indian Ocean to the Atlantic decreases. In the present conditions, the retroflection of a large portion of the Agulhas Current volume back to the Indian Ocean via the Agulhas Return Current (ARC). However, it is still unclear what impact the weakening of Agulhas leakage during the glacial period had on the oceanic environment in the Indian Ocean.

2. Results and discussions

We investigated several sediment cores from the western Indian sector of the Southern Ocean to reveal the oceanic frontal system changes during the glacial-interglacial time scale. The locations of sediment cores are across the Antarctic Polar Front (APF) and Subantarctic Front (SAF). We presented new sea-surface temperatures based on diatom census counts in several cores to infer past oceanographic changes. We also produced new sub-surface temperature datasets, based on a new transfer function method of radiolarian census counts (Civel-Mazens et al., 2023). In core MD11-3353, located in the Polar Front Zone (PFZ) west of Kerguelen Islands, both sea-surface and sub-surface temperatures follow the expected glacial-interglacial pattern, with a constant difference of ~3 °C, suggesting that the structure of the top 500 m of the water column did not change drastically over this period. In core MD12-3396CQ, located in the Subantarctic Zone (SAZ) east of Kerguelen Islands, the sub-surface temperature record again follows the expected glacial-interglacial pattern while the diatom-based reconstruction shows a strong warming during the 40-24 kyrs period, with a mean difference between the two of ~9 °C. The temperature difference subsequently reverts to ~3 °C during the glacial termination and Holocene. We suggest that the large difference between surface and sub-surface temperatures during the 40-24 kyrs period resulted from the injection of warm surface waters from the Indian low latitudes. This signal was transported to the core site by a strengthened Agulhas Return Current during the glacial, when the Agulhas leakage to the Atlantic was reduced (Civel-Mazens et al., 2021a). Our study thus proposes that the surface conditions in the SAZ are shaped by the interplay between the migration of the Southern Ocean hydrological fronts and the Agulhas (Return) Current, both being climatically modulated. We also reconstructed that the APF probably migrated south by ~5 degrees of latitude relative to its modern position during the warmer-than-present early interglacial periods (Marine Isotope Stage 5e and 7) (Civel-Mazens et al., 2021b).

References

Civel-Mazens, M., Cortese, G., Crosta, X., Lawler, K.A., Lowe, V., Ikehara, M., Itaki, T. (2023) New Southern Ocean transfer function for subsurface temperature prediction using radiolarian assemblages. *Marine Micropaleontology* **178**, 102198.

Civel-Mazens, M., Crosta, X., Cortese, G., Michel, E., Mazaud, A., Ther, O., Ikehara, M., Itaki, T. (2021a) Impact of the Agulhas Return Current on the oceanography of the Kerguelen Plateau region, Southern Ocean, over the last 40 kyrs. *Quaternary Science Reviews* **251**, 106711.

Civel-Mazens, M., Crosta, X., Cortese, G., Michel, E., Mazaud, A., Ther, O., Ikehara, M., Itaki, T. (2021b) Antarctic Polar Front migrations in the Kerguelen Plateau region, Southern Ocean, over the past 360 kyrs. *Global and Planetary Change* **202**, 103526.

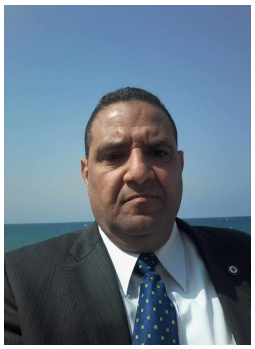

GEOHERITAGE MEANING OF PAST HUMIDITY IN THE CENTRAL WESTERN DESERT OF EGYPT

Fatma A. Mousa[1], Mohamed M. Abu El-Hassan[2], Hamdallah A. Wanasa[3], Emad S. Sallam[4], Vladimir A. Ermolaev[5], Dmitry A. Ruban[6]

1,2,3 Department of Geology, Faculty of Science, Menoufia University,Egypt

4 Department of Geology, Faculty of Science, Banha University, Egypt

5 Department of Commodity Science and Expertise, Plekhanov Russian University of Economics, Stremyanny Lane 36, Moscow 117997, Russia

6 Department of Organization and Technologies of Service Activities, Institute of Tourism, Service, and Creative Industries, Southern Federal University, Rostov-on-Don 344019, Russia. E-mail: ruban-d@mail.ru

1. Introduction

Geoheritage studies have become a consolidated branch of geosciences, with its own methods and nomenclature. Thematic geosites, means that several geosites from a given territory can be grouped by the common, rather narrow themes (frameworks sensu; Reynard & Brilha, 2018). Desert geoheritage has been reported from various places of the world, including the Atacama (Avaria, Donoso, & Barrientos, 2012). The Bahariya and Farafra oases are situated, boasts rich geology and have revealed the presence of highly-valuable geoheritage resource in this vast area (Abdel Maksoud, Baghdadi, & Ruban, 2021. The objective of the present contribution is to report the newly collected information about several unique Quaternary features. Based on new field investigations the issues of thematic geoheritage and geosite typology in the central Western Desert of Egypt and subsequent, novel interpretations of the collected information.

2. Results

A total of ten thematic localities in The Bahariya and Farafra oases can be summarized as follows. This thematic geoheritage represents chiefly carbonate rocks (calcretes, dolocretes, dolomites, travertines, and tufa) formed near springs, in streams and lakes (ponds), which existed temporary in the central Western Desert in the Pleistocene pluvial conditions. Cavernous carbonate rocks hosted aquifers formed under higher humidity, the discharge from which enabled surface hydrological systems to develop on slopes and local depressions and hollows.The humid climate facilitated karstification, including development of such a spectacular endokarst feature as the Djara Cave. Fluvial siliciclastics are found elsewhere in the area. There are also playas that mark desiccation of temporary ponds during desertification. The latter was responsible for the creation of phytogenic mounds (nebkha dunes). In several localities, sharp, unconformable contacts with pre-Quaternary sedimentary rocks are visible, which indicate on the start of the new phase of the regional geological evolution from the Pleistocene. Generally, the above-mentioned features reveal rather strong modification of the desert landscapes during Quaternary pluvial phases. The studied features allow the establishment of several geoheritage types, namely sedimentary, palaeogeographical, paleontological, mineralogical, stratigraphical, and geomorphological types. Taken together, they increase awareness of visitors about the Quaternary humidity in the central Western Desert.

3. Discussion

The thematic geoheritage (specific Quaternary environments) is found in ten localities. On the other hand, this theme is visible sharply in the entire regional geoheritage, although co-existing with some other geoheritage features. It is reasonable to propose that several geosites, which are equally important should be grouped, and combined in a "serial geosite". Such an operation is done in UNESCO World Heritage, and we suggest that it could be employed in such a situation as we have here. The geosite represents the relatively humid paleoclimate, which can be opposed to hyper-arid conditions, which have been typical to the study area in the Quaternary. The geological setting of this area implies that another geosite (Possibly, also serial) can be established there. Taking into account the studied geoheritage, it can be seen that the area has research significance on an international level. the proposed serial geosite can become essential for reconstructing the chronology of the paleoenvironmental fluctuations and, particularly, the Quaternary pluvial phases in the central Western Desert. Attention to this theme may facilitate distribution of the correct knowledge about climate changes, and, thus, contribute to the better awareness and understanding of the present and future climate changes.

References

Reynard, E., & Brilha, J. (2018). Geoheritage: Assessment, protection, and management. Amsterdam: Elsevier.

Avaria, C. C., Donoso, Á. Z., & Barrientos, C. P. (2012). Geomorphology and geoheritage of the Atacama Sand Sea Dunes, Copiapo (27o S), Chile. Revista de Geografia Norte Grande, 53, 123 – 136.

AbdelMaksoud, K.M., Baghdadi,M. I., & Ruban, D. A. (2021). Caves as geoheritage resource in remote desert areas: A preliminary evaluation of Djara Cave in theWesternDesert of Egypt. Geologos, 27(2), 105 – 113.

2023 Dec. 8					2023 Dec. 9			
9:00					9:00			
9:10					9:10			
9:20	Well come	Gad			9:20	12	Maher	Dawood
9:30	1	Gada El-Qady			9:30			
9:40					9:40			
9:50					9:50	13	AbdelHalin	Mahmoud
10:00					10:00			
10:10					10:10			
10:20	2	Mortada	El-Aref		10:20			
10:30					10:30	14	Kwame	FYNN
10:40					10:40			
10:50	3	Shoichi	Kiyokawa		10:50			
11:00					11:00	15	Ibrahim	Kwabina
11:10					11:10			
11:20					11:20			
11:30	4	FRANCOVS	Ion		11:30	16	Yoshimaru	Satoshi
11:40					11:40			
11:50					11:50			
12:00	Lunch				12:00	Lunch		
12:10					12:10			
12:20					12:20			
12:30					12:30			
12:40					12:40			
12:50					12:50			
13:00					13:00			
13:10		Tour of instute			13:10			
13:20					13:20	17	Motomura	Kento
13:30					13:30			
13:40	5	El Dokouny	Hanaa		13:40			
13:50					13:50			
14:00	6	David	Kuman		14:00	18	Hoffman	Axel
14:10					14:10	zoom		
14:20	7	Alex	Kovalick		14:20			
14:30					14:30			
14:40					14:40			
14:50					14:50	19	Hiroaki	Takahashi
15:00	8	Flávia	Braga	BR 10:00AM	15:00			
15:10	zoom			zoom	15:10	20	Fatma	Abdel Galil
15:20					15:20			
15:30					15:30			
15:40	9	Andrey	Bekker		15:40			
15:50					15:50	21	Minoru	Ikehara
16:00					16:00			
16:10				d	16:10			
16:20					16:20	22	ABOUELHA	Mohamed
16:30	10	Yusuke	Inokuchi		16:30			
16:40					16:40			
16:50	11	Mail	Ellithy		16:50	final	Shoichi	Kiyokawa
17:00					17:00			
17:10					17:10			
17:20					17:20			
17:30					17:30			
17:40					17:40			
17:50					17:50			
18:00					18:00			
18:30		Dinnar at			18:30		Dinnar at	
19:00					19:00			
19:30					19:30			
20:00					20:00			